



A novel catalyst Pd@ompg-C₃N₄ for highly chemoselective hydrogenation of quinoline under mild conditions

Yutong Gong, Pengfei Zhang, Xuan Xu, Yi Li, Haoran Li, Yong Wang*

Key Lab of Applied Chemistry of Zhejiang Province, Department of Chemistry, Zhejiang University, Hangzhou 310028, China

ARTICLE INFO

Article history:

Received 10 June 2012

Revised 16 October 2012

Accepted 17 October 2012

Available online 22 November 2012

Keywords:

Carbon nitride

Quinoline

Chemoselective hydrogenation

Heterogeneous catalyst

Mild condition

ABSTRACT

Polymeric mesoporous carbon graphitic nitrides (mpg-C₃N₄) and ordered mesoporous graphitic carbon nitrides (ompg-C₃N₄) with different surface area and morphology were used to prepare palladium catalysts (Pd@C₃N₄) by an easy ultrasonic-assisted method. These catalysts demonstrated excellent activity and selectivity for hydrogenation of quinoline to 1,2,3,4-tetrahydroquinoline under mild temperature (30–50 °C) and H₂ pressure (1 bar). Pd@ompg-C₃N₄ (*r* = 2.5) showed the best catalytic performance and both the activity and selectivity could be maintained for at least six reaction runs. The introduction of ordered cylindrical mesoporous structure and high concentration of surface Pd⁰ (about 70%) contribute to the high reaction activity and selectivity over Pd@ompg-C₃N₄ catalysts.

© 2012 Elsevier Inc. All rights reserved.

1. Introduction

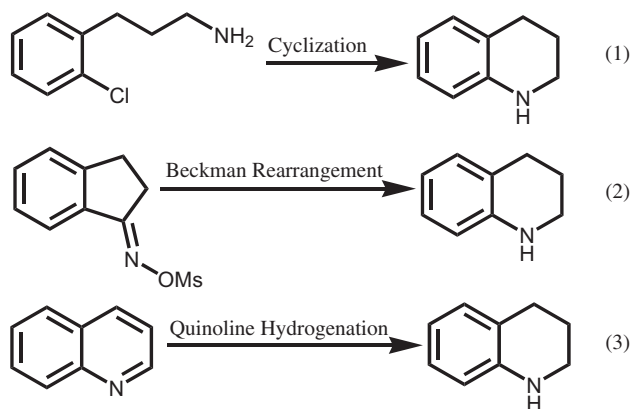
The synthesis of nitrogen heterocycles, including 1,2,3,4-tetrahydroquinoline (THQ), is of great current interest. THQ is an important intermediate for the synthesis of drugs, agrochemicals, dyes, alkaloids, and many other biological active molecules [1,2]. During recent decades, some catalytic methods have been established for the synthesis of THQ, such as the catalytic cyclization method [3,4], Beckman rearrangement [5], and the hydrogenation of quinoline (Scheme 1). Among these processes, direct selective hydrogenation of quinoline is widely regarded as the most convenient and most promising one owing to its high atom utilization together with easy access of the raw material.

Many homogeneous or heterogeneous metal catalysts can reduce isolated C=C, C=O and C=N double bonds in olefins, carbonyles, and imines, but hydrogenation of nitrogen-containing aromatics is more challenging [6,7]. Successful examples of the hydrogenation of quinoline by H₂ with homogeneous metal catalysts were firstly reported by Fish and coworkers in 1982 [8]. After that, homogeneous N-heterocycle hydrogenation, including quinoline hydrogenation, has proved possible with many Rh [9,10], Ru [11,12], Ir [13,14], and Os [15] catalysts precursors. Unfortunately, in most cases, the homogeneous catalysts displayed low activity under mild reaction conditions. Almost all quinoline hydrogenation catalysts require high pressures, elevated temperatures, or

long reaction time. For example, homogeneous Ir-based catalysts for the room temperature hydrogenation of quinolines typically require an excess of 15 bar of H₂ for high conversion, while catalysts that operate at lower hydrogen pressures require elevated temperatures (~100 °C or higher) [16,17]. Very recently, Crabtree and coworkers reported a new homogeneous Ir catalyst, which catalyzed hydrogenation of quinolines under mild conditions – as low as 1 bar of H₂ and 25 °C, however, after a long reaction time of 18 h [7]. Many homogeneous systems require the presence of harsh additives such as I₂, acid, or PPh₃ for good conversion or selectivity. In addition, the use of homogeneous metal catalysts on an industrial scale is limited by practical problems due to the difficulties in recovering the expensive catalyst metals, ligands, and additives from the reaction mixtures. In this context, the development of new and improved methods for the efficient and selective production of THQ continues to be a challenging goal. Heterogeneous catalysts especially supported precious metal catalysts have been drawing more and more attention for their superior reusability together with their outstanding catalytic performance [18]. However, only a few heterogeneous catalysts are available for the hydrogenation of quinoline to date, for example, Ru on poly(4-vinylpyridine) [19], Pd, Ru or Rh on Al₂O₃ [20], Ru on polyorganophosphazenes [21], Rh on montmorillonite [22], Pd on hydroxyapatites [23], and Pd on tannin-grafted collagen fibers [24]. Unfortunately, the complete conversion of quinoline to THQ with Ru-, Pd-, or Rh-based heterogeneous catalysts requires drastic reaction conditions, typically a temperature in the range of 60–200 °C, hydrogen pressure between 2.0 MPa and 4.0 MPa. As

* Corresponding author. Fax: +86 571 87951895.

E-mail address: chemwy@zju.edu.cn (Y. Wang).



Scheme 1. Synthetic routes to 1,2,3,4-tetrahydroquinoline.

a consequence, a highly effective heterogeneous catalyst under mild conditions is still desirable.

Carbon nitrides are fascinating materials that have attracted worldwide attention. They provide access to an even wider range of applications than carbon materials because the incorporation of nitrogen atoms in the carbon architecture can enhance the chemical, electrical, and functional properties. For example, our group and others have shown that a polymeric graphitic carbon nitride ($g\text{-C}_3\text{N}_4$), the most stable allotrope in the air, exhibits extreme chemical and thermal stability, can be chemically shaped to a variety of nanostructures, and can be directly used in heterogeneous catalysis [25–28], for example in oxidation of hydrocarbons [28–32]. However, few excellent applications as catalyst supports have emerged so far. We have recently disclosed a new strategy for the design of high-performance heterogeneous catalysts utilizing the $mpg\text{-C}_3\text{N}_4$ as catalyst support [18]. Highly dispersed palladium nanoparticles were introduced as a functional moiety into the $mpg\text{-C}_3\text{N}_4$ framework. The hybrid material, $\text{Pd}@mpg\text{-C}_3\text{N}_4$, exhibited promising catalytic performance for the selective hydrogenation of phenol. Considering the influence of diffusion steps in heterogeneous catalysis, metal nanoparticles loaded on ordered support bearing cylindrical pores would probably reveal better performance since substrates could reach the active sites more smoothly than on the support with random connected spherical pores. As part of our ongoing effort to develop new strategies for chemoselective hydrogenation, herein, we present the synthesis and characterization of the palladium-grafted ordered mesoporous carbon nitride ($\text{Pd}@omp\text{-C}_3\text{N}_4$) and employ it as an effective heterogeneous catalyst for the selective hydrogenation of quinoline by use of hydrogen under mild reaction conditions. We also mention the interesting aspects such as the pore structure effect and the substrate scope as well as the recycling of the catalyst.

2. Experimental

2.1. Materials and catalysts preparation

Ludox HS-40 silicon dispersion and SBA-15 were used as templates for the preparation of $mpg\text{-C}_3\text{N}_4$ and $omp\text{-C}_3\text{N}_4$, respectively. Ludox HS-40 with an average diameter of 12 nm was purchased from Sigma–Aldrich and used as received without any further treatment. $mpg\text{-C}_3\text{N}_4$ ($r = 1$, $r = M_{\text{LudoxHS-40}}/M_{\text{cyanamide}}$) was synthesized according to previous literature [33]. SBA-15 was synthesized according to a literature procedure [34]. Briefly, 8 g Pluronic P123 was dissolved in 240 ml 2 M HCl solution, and 17 g tetraethyl orthosilicate (TEOS) was added, and then the mixture was stirred at 35 °C for 20 h. The suspension was heated at 150 °C in a hydrothermal reactor for 48 h. After that, the resulting

mixture was filtered, washed by deionized water for several times, and dried in the air at room temperature. Finally, the dried white powder was calcined at 550 °C for 8 h. The above hydrothermally prepared SBA-15 was then used as a template for the preparation of $omp\text{-C}_3\text{N}_4$ [35,36]. 8 g of cyanamide, 2.5 ($r = 2.5$, $r = \text{weight of the used SBA-15 per 8 g cyanamide}$) g of SBA-15, and 20 g of deionized water were mixed together at room temperature and stirred for 1–2 h. Subsequently, the dispersion was filtrated and dried at 60 °C overnight until removal of water and formation of a white solid. The powder was then grounded in a mortar, transferred into a crucible, heated under air at 2.3 °C min^{-1} (4 h) up to 550 °C, and then treated at 550 °C for 4 h. The as-obtained yellow powder was ground in a mortar and then treated under stirring during 48 h in a 4 M NH_4HF_2 solution. The dispersion was then filtered, and then, the precipitate was washed with distilled water and ethanol. After filtering, the yellow compound was dried under vacuum at 100 °C overnight.

An ultrasonic-assisted method was applied to deposit Pd on $mpg\text{-C}_3\text{N}_4$ and $omp\text{-C}_3\text{N}_4$. Typically, 0.5 g $omp\text{-C}_3\text{N}_4$ ($r = 2.5$) was suspended in 50 ml deionized water, and the mixture was immersed into an ultrasonic instrument filled with water until $omp\text{-C}_3\text{N}_4$ was dispersed to a uniform suspension. After that, 10 ml of PdCl_2 aqueous solution (0.1 g/ml) was added into the $omp\text{-C}_3\text{N}_4$ suspension allowing the chelate adsorption of Pd^{2+} on $omp\text{-C}_3\text{N}_4$. 25 ml NaBH_4 aqueous solution (2 mg/ml) was added dropwise afterward, which would result in a grayish brown suspension. The slurry at last was filtered, washed with deionized water for several times, and dried in the air at 70 °C overnight. The resulting $\text{Pd}@omp\text{-C}_3\text{N}_4$ was then characterized by ICP, XRD, TEM, XPS, and BET, respectively.

2.2. Characterization analyses

Elemental analysis was performed by Elementar Vario MACRO. The Pd content was measured by ICP-AES (IRIS Intrepid II XSP, Thermo Fisher Scientific, USA). The surface areas of all the supports and catalyst were determined by AUTOSORB-1 instrument. BET equation was used to calculate the surface area and pore volume. Samples were outgassed at 100 °C for 20 h until the residual pressure was less than 10^{-4} Pa. The diffraction data were collected at room temperature with 2θ scan range between 5° and 90° using a wide-angle X-ray diffraction (Model D/tex-Ultima TV, 1.6 kV, Rigaku, Japan) equipped with Cu K α radiation (1.54 Å). The X-ray photoelectron spectra were obtained with an ESCALAB MARK II spherical analyzer using a magnesium anode (Mg 1253.6 eV) X-ray source. The powder samples were pressed to pellets and fixed to a stainless steel sample holder without further treatment. The XPS spectrum was shifted according to C_{1s} peak being at 288.2 eV so as to correct the charging effect [18]. TEM (Model JEM-1230, JEOL Co. Ltd., Japan) characterization was operated at an accelerating voltage of 80 kV. FTIR was measured by Bruker Vector 22. Benzene-TPD and pyridine-TPD were conducted as follows: 0.1 g of dry $omp\text{-C}_3\text{N}_4$ ($r = 2.5$) was mixed with quartz sand and placed into a quartz tube located inside an electrical furnace. Then, benzene or pyridine was brought into the tube by He for 1 h. The samples were blown by pure He for about 2 h until no change of TCD signal next. At last, the electrical furnace was subjected to a 10 °C/min heating rate up to 400 °C, under a He flow of 40 cm^3/min . The desorption of benzene and pyridine was monitored by a thermal conductivity detector.

2.3. Catalytic procedure and recycling

The hydrogenation of quinoline using hydrogen was carried out in a batch-type reactor operated under atmospheric conditions. Experiments were conducted using a three necked glass flask (capacity 25 ml) precharged with quinoline, solvent, and catalyst.

The mixture was stirred using a magnetic stirrer and heated in a water bath. The system was equipped with a thermocouple to control the temperature and a reflux condenser. The reactor was sealed and purged with H₂ to remove the air for three times and then equipped with a hydrogen balloon. Samples were taken between certain time intervals and analyzed using a Shimadzu GC-2014 gas chromatograph equipped with a Rtx-1071 column. Decane was used as an internal standard to calculate quinoline conversion and THQ selectivity. The GC conditions for the product analysis were as follows: Injector Port Temperature: 260 °C; Column Temperature: Initial temperature: 60 °C (1 min); Gradient Rate: 50 °C/min (3.8 min); Final Temperature: 250 °C (10 min). The catalyst used above was recovered by centrifugation, washed three times with ethanol, and dried at 80 °C for 6 h. The slight loss of catalyst was replenished by new catalyst without changes of other conditions for the next cycle.

3. Results and discussion

3.1. Catalyst characterization

Elemental analysis of mpg- and ompg-C₃N₄ results are shown in Table S1 (Supporting information), and all these supports give a C/N ratio around 0.68. The residual H contents attributable to incomplete condensation or adsorbed water vary from 2.75 W% to 3.10 W%. To understand the textural properties, the mpg-C₃N₄ and ompg-C₃N₄ supports prepared under different conditions and the Pd@ompg-C₃N₄(*r* = 2.5) catalyst were characterized by N₂ adsorption–desorption measurements. The isotherms and the Barrett–Joyner–Halenda (BJH) pore size distributions are shown

Table 1

Textural properties of mpg-C₃N₄, ompg-C₃N₄, active carbon and Pd@ompg-C₃N₄.

Entry	Support or catalyst	<i>S</i> _{BET} ^a (m ² /g)	<i>P</i> _v ^b (cm ³ /g)	<i>P</i> _s ^c (nm)
1	mpg-C ₃ N ₄ (<i>r</i> = 1)	148	0.52	9.4
2	ompg-C ₃ N ₄ (<i>r</i> = 1)	142	0.28	6.07
3	ompg-C ₃ N ₄ (<i>r</i> = 1.5)	198	0.44	7.17
4	ompg-C ₃ N ₄ (<i>r</i> = 2.5)	212	0.48	7.42
5	active carbon	899	0.64	4.58
6	Pd@ompg-C ₃ N ₄ (<i>r</i> = 2.5)	197	0.32	5.68

All were determined from the desorption branch of the nitrogen.

^a BET surface area.

^b Pore volume.

^c Pore size.

in Fig. 1. N₂ adsorption–desorption isotherm curves of these samples show a pronounced hysteresis, typical of the existence of mesopore structures, only weak microporosity. The Brunauer–Emmett–Teller (BET) surface area, BJH pore sizes, and pore volumes are summarized in Table 1. The BET surface area (as determined from the desorption branch of the nitrogen) are between 142 m² g^{−1} and 212 m² g^{−1}, depending on the weight fraction of the template. In Fig. 1c, nitrogen adsorption isotherms of the parent ompg-C₃N₄(*r* = 2.5) and modified Pd@ompg-C₃N₄(*r* = 2.5) material are also presented. After the modification, the isotherm shape was preserved, indicating that the Pd nanoparticles do not block or alter the pore system.

The Pd loading after modification was analyzed by ICP-AES and listed in Table 2. All the actual Pd loadings for the prepared four catalysts are slightly less than the expected 10 w%, but the loadings of Pd do not differ much on the four different kinds of C₃N₄ as shown in Table 2.

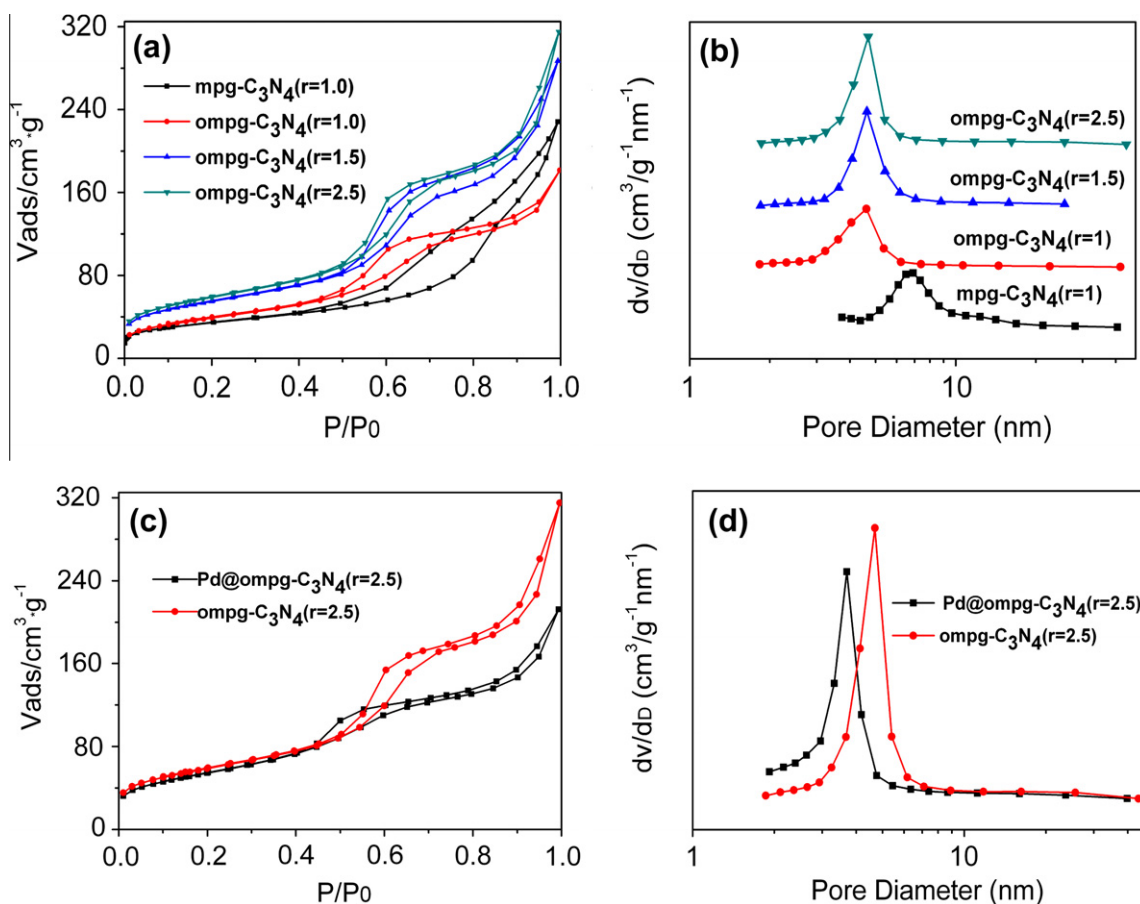


Fig. 1. N₂ adsorption/desorption isotherms of C₃N₄s (a), Pd@ompg-C₃N₄ (*r* = 2.5) (c) and corresponding Barrett–Joyner–Halenda (BJH) pore-size distribution curve (b), (d) determined from the desorption branch.

Table 2
Pd loadings on four C₃N₄ supports and active carbon.

Entry	Catalyst	Pd loading (wt%)
1	Pd@ompg-C ₃ N ₄ (<i>r</i> = 1)	9.48
2	Pd@ompg-C ₃ N ₄ (<i>r</i> = 1.5)	9.52
3	Pd@ompg-C ₃ N ₄ (<i>r</i> = 2.5)	9.33
4	Pd@mpg-C ₃ N ₄ (<i>r</i> = 1)	9.55
5	Pd@C	9.04

The small-angle XRD patterns of mpg-C₃N₄, ompg-C₃N₄, and SBA-15 are shown in Fig. S1 (Supporting information). The pattern of SBA-15 shows three well-resolved peaks, which can be assigned to the (100), (110), (200) diffractions of a 2D hexagonal pore structure with p6mm symmetry. The ompg-C₃N₄ pattern shows a similar form, proving a perfect replication of the SBA-15-ordered pore structure. However, there is no obvious peak for mpg-C₃N₄, which is an evidence of a disordered pore system. The wide-angle XRD patterns of ompg-C₃N₄ and Pd@ompg-C₃N₄ are shown in Fig. 2a. A diffraction peak at 27.3° is observed for both of the

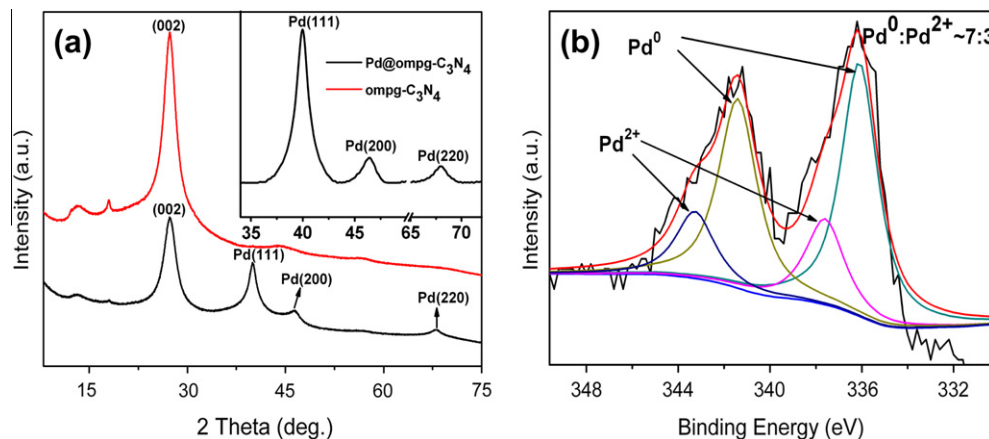


Fig. 2. XRD patterns of ompg-C₃N₄(*r* = 2.5) and Pd@ompg-C₃N₄(*r* = 2.5) (a) and XPS pattern of ompg-C₃N₄(*r* = 2.5) (b).

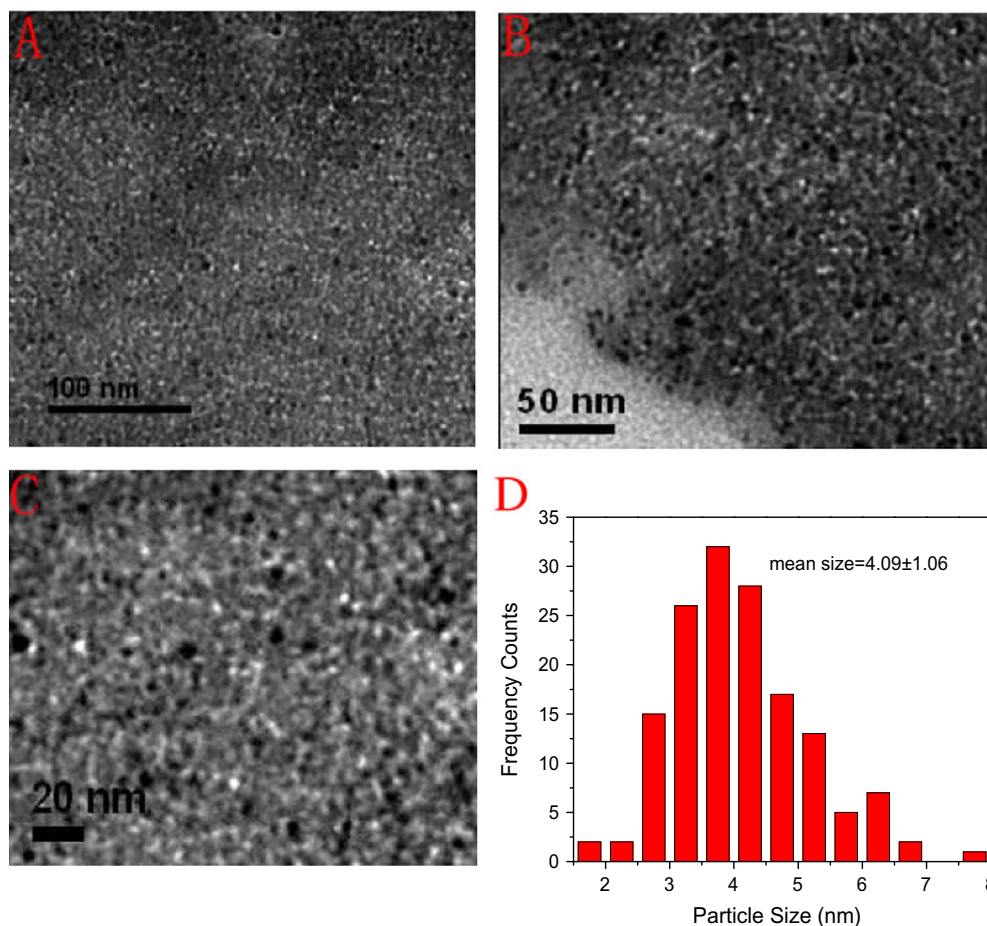
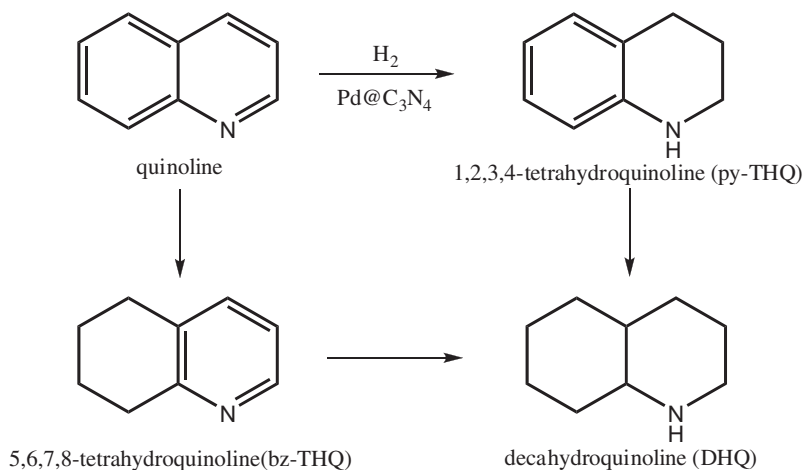


Fig. 3. TEM images of 10wtPd@ompg-C₃N₄(*r* = 2.5) with different magnification (A–C) and size distribution of Pd particles (D).



Scheme 2. Possible reaction pathways for quinoline hydrogenation.

samples and ascribed to the characteristic peak of (002) packing of $g\text{-C}_3\text{N}_4$. The diffraction peaks at 40.0° , 46.6° , and 68.1° in the XRD patterns can be assigned to the (111), (200), and (220) planes of Pd metal particles, respectively. The average size of the crystallites was calculated to be 5.4 nm from the major diffraction peak (111) using Scherrer's formula. The morphologies of Pd@omp- C_3N_4 composite materials were also investigated by TEM (Fig. 3). The TEM images revealed well-dispersed Pd particles with a mean size of 4.1 nm (Fig. 3D), which is smaller than that calculated from XRD results. XPS was then applied to identify the surface composition and oxidation state of Pd species. Fig. 2b shows the XPS spectra in the Pd 3d binding energy region of Pd@omp- C_3N_4 ($r = 2.5$). Two peaks that appear at 341.3 eV and 336.1 eV are related to Pd^0 3d_{3/2} and Pd^0 3d_{5/2}, while peaks at 343.1 eV and 337.6 eV are attributed to Pd^{2+} 3d_{3/2} and Pd^{2+} 3d_{5/2}. The percentage of the Pd^0 and Pd^{2+} species was calculated from the relative areas of these peaks. It indicates that Pd^0 is the main metal species on the surface of the as-prepared catalyst (~70%), which is consistent with Pd@mpg- C_3N_4 as clarified in our previous work [18]. The catalytic activity of precious metals supported on carbon material is highly dependent on the nature of surface functional groups present on the support. Indeed, support (carbon carriers) modification with acidic oxygen-containing and basic nitrogen-containing surface groups is already widely performed [37–39]. For example, Radkevich and coworkers proved the presence of amine groups in the carbon carrier helped stabilize Pd^0 in a high-dispersed state and resulted in increased proportion of Pd^0 , resistant to reoxidation [40]. In our case, omp- C_3N_4 has a high nitrogen content of 53 wt%. The π -bonded planar C–N–C-layers along with the incompletely condensed amino groups (Supporting information, Fig. S2) in the omp- C_3N_4 are suitable for stabilizing highly dispersed Pd^0 particles, preventing their reoxidation and improving their activity in hydrogen activation.

3.2. Hydrogenation of quinoline

Quinoline hydrogenation ideally involves the regioselective hydrogenation of the nitrogen-containing ring to form py-THQ. However, the complete hydrogenation product decahydroquinoline (DHQ) and the benzene ring hydrogenation product 5,6,7,8-tetrahydroquinoline (bz-THQ) may also form during the reaction process (Scheme 2). For example, commercial Pd/C catalyst only gave an 84% selectivity toward py-THQ [24].

3.2.1. The effect of solvents

In order to investigate the catalytic response of Pd@ C_3N_4 (including Pd@mpg- C_3N_4 and Pd@omp- C_3N_4) in quinoline hydro-

Table 3

Conversion of quinoline in different solvents.

Entry	Solvent	Conv. (%) ^a	Sel. (%) ^a
1	Ethanol	82	100
2	Water	32	100
3	Acetonitrile	99	99
4	Methanol	80	100
5	Toluene	86	100
6	Tetrahydrofuran	57	100
7	n-Hexane	76	100

Reaction conditions: quinoline (0.5 mmol), Pd (4.7 mol% relative to quinoline), 5 ml solvent, using Pd@omp- C_3N_4 ($r = 1$).

^a Determined by GC and GC-MS.

genation, we selected Pd@omp- C_3N_4 ($r = 1$) as catalyst and tested its reaction activity in several solvents. As demonstrated in Table 3, Pd@omp- C_3N_4 promoted the exclusive formation of py-THQ with no evidence of benzene ring reduction or complete hydrogenation, that is, exclusive nitrogen-containing ring hydrogenation, which confirms the high selectivity of the as-prepared Pd@omp- C_3N_4 . With Pd@omp- C_3N_4 ($r = 1$) under the primary conditions, we could readily achieve 100% selectivity toward py-THQ, with a conversion of quinoline of 32–86% in 4 h at 30 °C and 1 bar of hydrogen pressure (Table 3). In homogeneous catalysis systems, the electronic properties of the solvent can alter the mechanistic aspects of a reaction via a change in the free energy state of the reactants, which can alter the favorability of different reaction paths [41]. With heterogeneous catalysts, the solvation of reacting species and its impact on the overall reaction mechanism are not clearly understood [42]. However, in a study of polar and nonpolar reactants, it has been stated that hydrogenation of less polar substrates in more polar solvents is preferred [43,44]. Note that in our reaction systems, the reaction rates were affected by the choice of solvents. However, no difference was observed in selectivity in different solvents. Table 3 indicates that the conversion of quinoline after 4 h in the different solvents decreased in the following order: acetonitrile > toluene > ethanol > methanol > n-hexane > tetrahydrofuran > water. In this case, it was found that the variation in specific activity did not correlate with either the solvent dielectric constant, polarity, or the dipole moment (Supporting information, Fig. S3). This phenomenon was also observed in the hydrogenation of citral using Pt/SiO₂, and the reason has been attributed to the higher multipole moments of some solvents [44]. Acetonitrile gave the highest activity but itself would be hydrogenated to triethylamine under harsh reaction conditions. In addition, considering the toxicity of acetonitrile and toluene, we

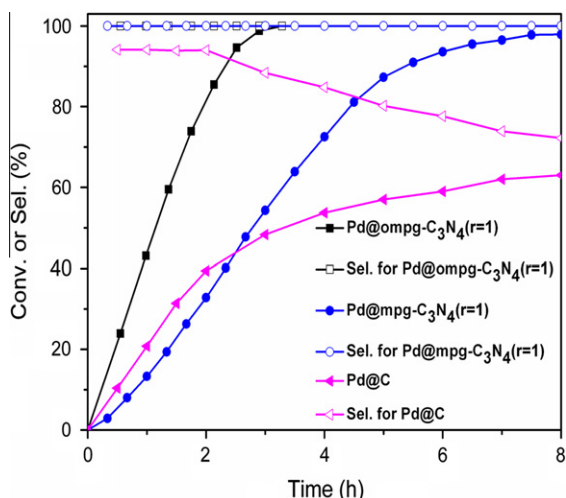


Fig. 4. 1,2,3,4-Tetrahydroquinoline yield as a function of time at 40 °C using 5 ml ethanol as solvent over 25 mg Pd@mpg-C₃N₄(r = 1), Pd@ompg-C₃N₄(r = 1) and 27 mg Pd@C.

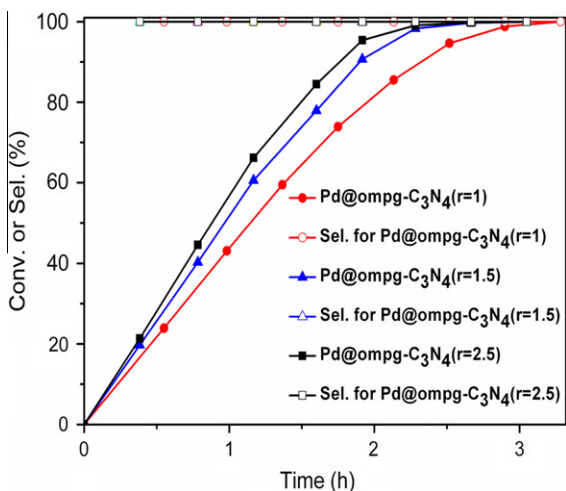
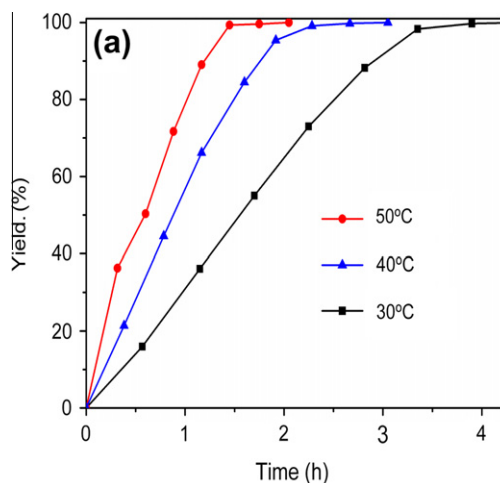


Fig. 5. 1,2,3,4-Tetrahydroquinoline yield as a function of time at 40 °C using 5 ml ethanol as solvent over Pd@ompg-C₃N₄.



afterward limited the subsequent catalytic study in an ethanol solvent feed at 1 bar of hydrogen pressure.

3.2.2. The effect of textural properties

In effort to compare the potential abilities of Pd@C₃N₄ with different textural properties, the conversions of quinoline as a function of reaction time over different Pd@C₃N₄ catalyst are presented in Fig. 4. For comparison, the reaction result with Pd@C as catalyst is also listed in the figure. It can be observed that Pd@ompg-C₃N₄(r = 1) exhibited the highest activity among the tested three catalysts. Yet, Pd@mpg-C₃N₄ showed an activity between that of the Pd@ompg-C₃N₄ and Pd@C. The reduction in quinoline using Pd@ompg-C₃N₄(r = 1) led to a 100% conversion in 100% selectivity toward py-THQ at 40 °C in 3 h, and a similar Pd@mpg-C₃N₄ catalyst gave a 54% conversion (100% selectivity) under the same reaction conditions. In comparison, the reaction performed using Pd@C as catalyst gave a 48% conversion and only 88% selectivity toward py-THQ. The selectivity to py-THQ remained 100% on Pd@C₃N₄ catalysts even the conversion reached 100%, but decreased markedly on the Pd@C catalyst. The superior activity of Pd@C₃N₄ can be attributed to the high nitrogen content in the carbon nitride carrier resulting in increased proportions of Pd⁰, which was reported as the active site for the activation of H₂ [18,40]. Pd@Al₂O₃ was reported to show very good activity and selectivity in the hydrogenation of quinoline under relatively harsher conditions (>100 °C, 2 MPa H₂) [20], however, under our mild reaction conditions (40 °C, 1 bar H₂), only minor py-THQ was observed (Supporting information, Fig. S6).

Pd@ompg-C₃N₄ catalysts show much higher efficiency than Pd@mpg-C₃N₄. The advantage of using ompg-C₃N₄ can attribute to the uniform cylindrical pores. The character allows substrates to diffuse to the active sites with relatively less barriers. While in the case of mpg-C₃N₄, the spherical pores are just connected by random smaller bottlenecks which will hinder mass transfer in all directions [27,35]. A comparative study of Pd@ompg-C₃N₄(r = 1), Pd@ompg-C₃N₄(r = 1.5) and Pd@ompg-C₃N₄(r = 2.5) was then carried out. As shown in Fig. 5, apparently different surface area and pore size exhibit a significant influence in activity, for example, with Pd@ompg-C₃N₄(r = 2.5) as catalyst, the reaction completed in 2.5 h with 100% selectivity toward py-THQ which is much faster than that using Pd@ompg-C₃N₄(r = 1) as catalyst.

3.2.3. The influence of temperature

Variation of the reaction temperature had a considerable effect on the reaction conversion, as illustrated in Fig. 6. Conversion of

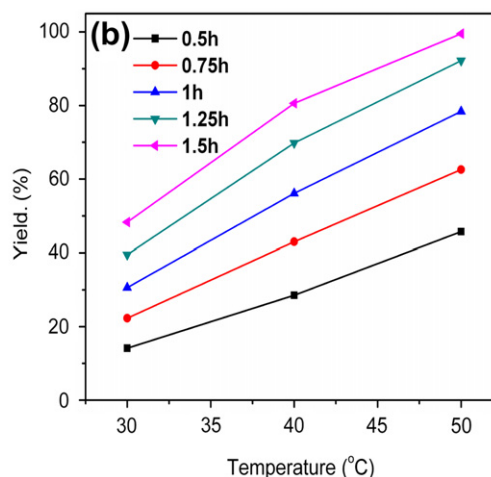


Fig. 6. 1,2,3,4-Tetrahydroquinoline yield as a function of time (a) and temperature (b) using 5 ml ethanol as solvent over 25 mg Pd@ompg-C₃N₄(r = 2.5) at different temperature and time.

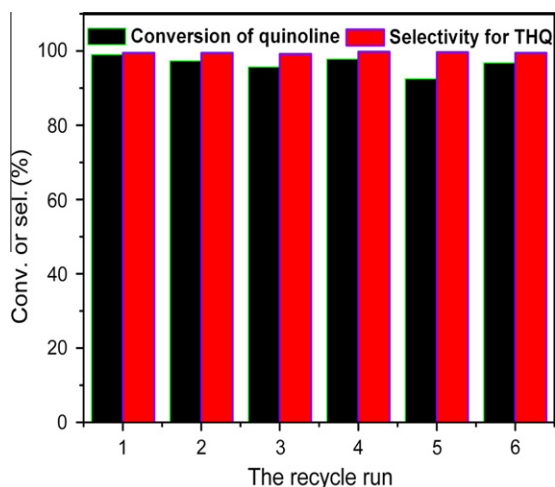


Fig. 7. Reuse of Pd@omp-g-C₃N₄(*r* = 2.5) under 40 °C for 2.5 h.

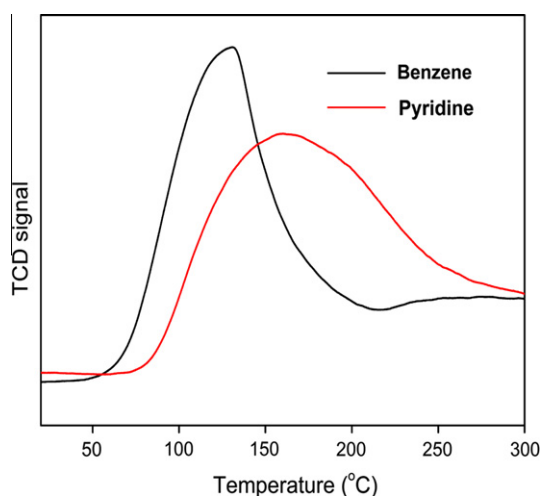


Fig. 8. TPD profiles of benzene and pyridine.

100% was achieved with a 100% selectivity within 2.5 h at 1 bar of hydrogen pressure and 40 °C. The reaction was accelerated at higher temperature but without any losing of the selectivity, for example, full conversion in 1.5 h was obtained at 50 °C with a high selectivity of 100%. But, even at a low temperature of 30 °C, 100% conversion and 100% selectivity could be reached after a minor longer reaction time of 4 h. Hydrogenation under mild conditions is extremely desirable in industry.

3.2.4. The reusability of the catalyst

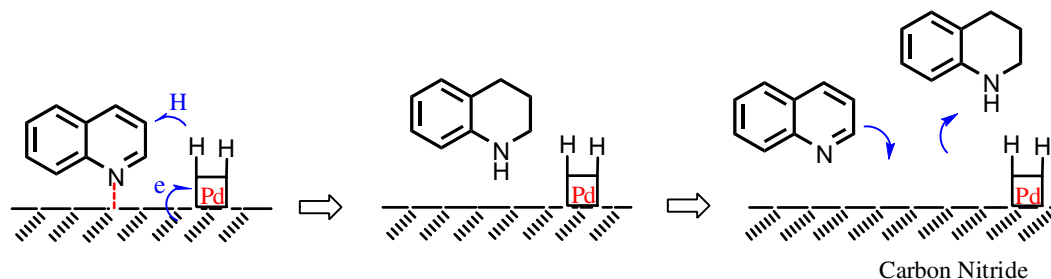
It has been reported that the commercial Pd@C lost its activity in quinoline hydrogenation after used for 3 times [24]. We then

investigated the recyclability of the Pd@omp-g-C₃N₄(*r* = 2.5) catalyst. Fig. 7 gives the results of catalyst recycling at 40 °C in ethanol. The Pd@omp-g-C₃N₄(*r* = 2.5) was able to recycle at least six times without significant loss of activity, which is a prerequisite for practical applications. Highly dispersed Pd⁰ clusters are capable of reoxidation during air (or oxygen) contact which may lead to the deactivation of the catalysts [45]. However, our catalysts are very stable in the air and the samples can be stored in air at room temperature for several months without loss of their activities.

3.2.5. Possible mechanism

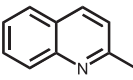
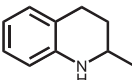
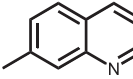
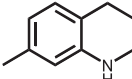
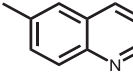
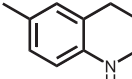
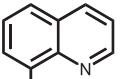
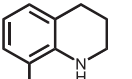
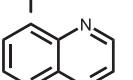
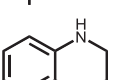
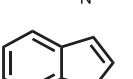
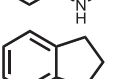
Py-THQ was the only reaction product observed over the entire range of conditions studied, which suggests that the hydrogenation of quinoline is going via the exclusive adsorption of N-heterocycle part [46–48]. To specifically explain the exclusive adsorption behaviors is difficult, but depending on the nature of the catalyst's active site, quinoline can interact with the surface through the N-heterocycle to form strong N···H–N interactions or π···π interactions. Both our group and others have demonstrated the efficient use of the NH and NH₂ groups on the surface of carbon nitride for the effective adsorption of phenol via O···H–N or O–H···N interactions recently [18,49]. Similar to this result, although an interaction between the aromatic ring of quinoline and the π electron of the carbon nitride could not be excluded, we expect that such a π···π interaction is weaker and quinoline adsorbs on the carbon nitride mainly via a N···H–N interaction. This conclusion is supported by the TPD experiments. TPD experiments of benzene and pyridine were conducted, and the results were displayed in Fig. 8. Desorption of pyridine from C₃N₄ started at around 75 °C, and it exhibited a maximum desorption rate at about 161 °C. While for benzene, the temperatures for initial desorption and maximum desorption rate located at 50 °C and 130 °C, respectively. The results demonstrate that the binding energy of pyridine with C₃N₄ is higher than that of benzene with C₃N₄. It indicates that the incorporation of nitrogen atom increases the interaction between pyridine and C₃N₄. Similarly, pyridine ring of quinoline in principal possesses higher bonding energy with C₃N₄ than benzene ring. This stronger interaction may account for the high selectivity for 1,2,3,4-tetrahydroquinoline.

The transfer of electron density in the heterojunction from the semiconductor C₃N₄ enriches the electron density of the metallic Pd and accelerates the hydrogenation reaction, as compared to Pd@C. Scheme 3 illustrates the proposed step sequence of the hydrogenation of quinoline. In the initial stage, the adsorption of N-heterocycle of quinoline onto the carbon nitride support is significantly promoted by the formation of N···H–N hydrogen bonds between the N-heterocycle of quinoline molecule and the NH and NH₂ groups on the surface of carbon nitride. Subsequently, those quinoline molecules interacted with the active H produced over Pd nanoparticles, resulting in the formation of py-THQ. That the product of quinoline hydrogenation is depended on the adsorption types of quinoline over the catalyst had already been studied in detail by Fish et al. [46], and improved selectivity toward the



Scheme 3. Possible reaction mechanism of quinoline hydrogenation over Pd@C₃N₄.

Table 4
Hydrogenation of other quinolines and 2,3-benzofuran.

Substrates	Product	Solvent	Temperature (°C)	Time (h)	Conv. ^a (%)	Sel. ^a (%)
		Ethanol	60	5	>99	95
		Ethanol	60	2	>99	>99
		Toluene	100	2	>99	>99
		Toluene	100	1	>99	>99
		Ethanol	40	3	80	95
		Ethanol	40	5	>99	>99

Reaction conditions: 0.5 mmol substrate, 4.7 mol%Pd, 5 ml solvent, unless otherwise noted.

^a Determined by GC and GC-MS.

formation of py-THQ via hydrogen bonds was also observed by Shi and coworkers [24].

3.2.6. Test for other quinolines

Furthermore, the applicability of Pd@ompg-C₃N₄ ($r = 2.5$) catalyst to different heterocyclic compounds was investigated, and the results are summarized in Table 4. The reactions were retarded when methyl group was introduced. Therefore, a little higher temperature is needed for the hydrogenation of substituted quinolines to corresponding 1,2,3,4-tetrahydroquinolines smoothly. 2,3-Benzofuran was used to test if this kind of catalyst is also highly effective for hydrogenation of oxygen heterocyclic compounds. To our delight, the catalyst actually showed high activity and selectivity toward the reduction of 2,3-benzofuran as demonstrated in Table 4.

4. Conclusions

Mpg-C₃N₄ and ompg-C₃N₄ were successfully synthesized, and Pd was subsequently deposited by an easy ultrasonic-assisted method, leading to the formation of highly dispersed Pd nanoparticles. The polymeric C₃N₄ supports, especially the ompg-C₃N₄ remarkably enhanced both the catalytic activity and the selectivity in the hydrogenation of quinoline with molecular hydrogen as a reductant, compared with the active carbon. Recycling experiment of Pd@ompg-C₃N₄ indicated that the catalyst could be reused for more than six times without significant loss of catalytic activity and selectivity. The enhanced catalytic activity can be attributed to synergetic interaction between Pd and C₃N₄ supports, the π -bonded planar C–N–C layers along with the incompletely condensed amino groups in the carbon nitride are suitable for stabilizing highly dispersed Pd⁰ particles. Good accessibility of Pd active sites and high concentration of surface Pd⁰ contribute to the high reaction activity over C₃N₄-supported Pd catalysts. The introduction of ordered cylindrical mesoporous structure may facilitate mass transfer and therefore lead to better catalytic performance.

Acknowledgments

We thank Prof. M. Antonietti for helpful discussion. Financial support from the Joint Petroleum and Petrochemical Funds of the National Natural Science Foundation of China and China National Petroleum Corporation (U1162124), the Fundamental Research Funds for the Central Universities, the Program for Zhejiang Leading Team of S&T Innovation (2011R50007), and the Partner Group Program of the Zhejiang University and the Max-Planck Society are greatly appreciated.

Appendix A. Supplementary data

Supplementary data associated with this article can be found, in the online version, at <http://dx.doi.org/10.1016/j.jcat.2012.10.018>. These data include MOL files and InChIKeys of the most important compounds described in this article.

References

- [1] R.T. Shuman, P.L. Ornstein, J.W. Paschal, P.D. Gesellchen, *J. Org. Chem.* 55 (1990) 738.
- [2] A.R. Katritzky, S. Rachwal, B. Rachwal, *Tetrahedron* 52 (1996) 15031.
- [3] R. Omar-Amrani, A. Thomas, E. Brenner, R. Schneider, *Y. Fort, Org. Lett.* 5 (2003) 2311.
- [4] T. Kubo, C. Katoh, K. Yamada, K. Okano, H. Tokuyama, T. Fukuyama, *Tetrahedron* 64 (2008) 11230.
- [5] K. Maruoka, T. Miyazaki, M. Ando, Y. Matsumura, S. Sakane, K. Hattori, H. Yamamoto, *J. Am. Chem. Soc.* 105 (1983) 2831.
- [6] Y.G. Zhou, *Acc. Chem. Res.* 40 (2007) 1357.
- [7] G.E. Dobreiner, A. Nova, N.D. Schley, N. Hazari, S.J. Miller, O. Eisenstein, R.H. Crabtree, *J. Am. Chem. Soc.* 133 (2011) 7547.
- [8] R.H. Fish, A.D. Thormodsén, G.A. Cremer, *J. Am. Chem. Soc.* 104 (1982) 5234.
- [9] Y. Alvarado, M. Busolo, F. Lopez-Linares, *J. Mol. Catal. A: Chem.* 142 (1999) 163.
- [10] M. Rosales, L.J. Bastidas, B. Gonzalez, R. Vallejo, P.J. Baricelli, *Catal. Lett.* 141 (2011) 1305.
- [11] S.M. Lu, X.W. Han, Y.G. Zhou, *J. Organomet. Chem.* 692 (2007) 3065.
- [12] Z.J. Wang, H.F. Zhou, T.L. Wang, Y.M. He, Q.H. Fan, *Green Chem.* 11 (2009) 767.
- [13] W.B. Wang, S.M. Lu, P.Y. Yang, X.W. Han, Y.G. Zhou, *J. Am. Chem. Soc.* 125 (2003) 10536.
- [14] S.M. Lu, X.W. Han, Y.G. Zhou, *Adv. Synth. Catal.* 346 (2004) 909.
- [15] M. Rosales, S. Castillo, A. Gonzalez, L. Gonzalez, K. Molina, J. Navarro, I. Pacheco, H. Perez, *Transition Met. Chem.* 29 (2004) 221.

- [16] R. Yamaguchi, C. Ikeda, Y. Takahashi, K. Fujita, *J. Am. Chem. Soc.* 131 (2009) 8410.
- [17] R.A. Sanchezdelgado, D. Rondon, A. Andriollo, V. Herrera, G. Martin, B. Chaudret, *Organometallics* 12 (1993) 4291.
- [18] Y. Wang, J. Yao, H.R. Li, D.S. Su, M. Antonietti, *J. Am. Chem. Soc.* 133 (2011) 2362.
- [19] R.A. Sanchez-Delgado, N. Machalaba, N. Ng-A-Qui, *Catal. Commun.* 8 (2007) 2115.
- [20] M. Campanati, A. Vaccari, O. Piccolo, *J. Mol. Catal. A: Chem.* 179 (2002) 287.
- [21] A. Spitaleri, P. Pertici, N. Scalera, G. Vitulli, M. Hoang, T.W. Turney, M. Gleria, *Inorg. Chim. Acta* 352 (2003) 61.
- [22] M. Campanati, M. Casagrande, I. Fagiolino, M. Lenarda, L. Storaro, M. Battagliarin, A. Vaccari, *J. Mol. Catal. A: Chem.* 184 (2002) 267.
- [23] N. Hashimoto, Y. Takahashi, T. Hara, S. Shimazu, T. Mitsudome, T. Mizugaki, K. Jitsukawa, K. Kaneda, *Chem. Lett.* 39 (2010) 832.
- [24] H. Mao, C. Chen, X.P. Liao, B. Shi, *J. Mol. Catal. A: Chem.* 341 (2011) 51.
- [25] Y. Wang, X.C. Wang, M. Antonietti, *Angew. Chem. Int. Ed.* 51 (2012) 68.
- [26] A. Thomas, A. Fischer, F. Goettmann, M. Antonietti, J.O. Muller, R. Schlögl, J.M. Carlsson, *J. Mater. Chem.* 18 (2008) 4893.
- [27] X. Jin, V.V. Balasubramanian, S.T. Selvan, D.P. Sawant, M.A. Chari, G.Q. Lu, A. Vinu, *Angew. Chem. Int. Ed.* 48 (2009) 7884.
- [28] J.J. Zhu, S.A.C. Carabineiro, D. Shan, J.L. Faria, Y.J. Zhu, J.L. Figueiredo, *J. Catal.* 274 (2010) 207.
- [29] Y. Wang, Y. Di, M. Antonietti, H.R. Li, X.F. Chen, X.C. Wang, *Chem. Mater.* 22 (2010) 5119.
- [30] Y. Wang, J.S. Zhang, X.C. Wang, M. Antonietti, H.R. Li, *Angew. Chem. Int. Ed.* 49 (2010) 3356.
- [31] Y. Wang, H.R. Li, J. Yao, X.C. Wang, M. Antonietti, *Chem. Sci.* 2 (2011) 446.
- [32] P.F. Zhang, Y. Wang, J. Yao, C.M. Wang, C. Yan, M. Antonietti, H.R. Li, *Adv. Synth. Catal.* 353 (2011) 1447.
- [33] F. Goettmann, A. Fischer, M. Antonietti, A. Thomas, *Angew. Chem. Int. Ed.* 45 (2006) 4467.
- [34] D.Y. Zhao, Q.S. Huo, J.L. Feng, B.F. Chmelka, G.D. Stucky, *J. Am. Chem. Soc.* 120 (1998) 6024.
- [35] X.F. Chen, Y.S. Jun, K. Takanabe, K. Maeda, K. Domen, X.Z. Fu, M. Antonietti, X.C. Wang, *Chem. Mater.* 21 (2009) 4093.
- [36] Y.S. Jun, W.H. Hong, M. Antonietti, A. Thomas, *Adv. Mater.* 21 (2009) 4270.
- [37] D.A. Bulushev, I. Yuranov, E.I. Suvorova, P.A. Buffat, L. Kiwi-Minsker, *J. Catal.* 224 (2004) 8.
- [38] S. Hermans, C. Diverchy, O. Demoulin, V. Dubois, E.M. Gaigneaux, M. Devillers, *J. Catal.* 243 (2006) 239.
- [39] M. Gurrath, T. Kuretzky, H.P. Boehm, L.B. Okhlopkova, A.S. Lisitsyn, V.A. Likholobov, *Carbon* 38 (2000) 1241.
- [40] V.Z. Radkevich, T.L. Senko, K. Wilson, L.M. Grishenko, A.N. Zaderko, V.Y. Diyuk, *Appl. Catal. A – Gen.* 335 (2008) 241.
- [41] M.H. Abraham, P.L. Grellier, J.L.M. Abboud, R.M. Doherty, R.W. Taft, *Can. J. Chem. – Rev. Can. Chim.* 66 (1988) 2673.
- [42] B.S. Akpa, C. D'Agostino, L.F. Gadden, K. Hindle, H. Manyar, J. McGregor, R. Li, M. Neurock, N. Sinha, E.H. Stitt, D. Weber, J.A. Zeitler, D.W. Rooney, *J. Catal.* 289 (2012) 30.
- [43] R.A. Rajadhyaksha, S.L. Karwa, *Chem. Eng. Sci.* 41 (1986) 1765.
- [44] S. Mukherjee, M.A. Vannice, *J. Catal.* 243 (2006) 108.
- [45] M.V. Klyuev, A.A. Nasibulin, *Kinet. Catal. (Russia)* 37 (1996) 231.
- [46] E. Baralt, S.J. Smith, J. Hurwitz, I.T. Horvath, R.H. Fish, *J. Am. Chem. Soc.* 114 (1992) 5187.
- [47] R.H. Fish, E. Baralt, H.S. Kim, *Organometallics* 10 (1991) 1965.
- [48] R.H. Fish, J.N. Michaels, R.S. Moore, H. Heinemann, *J. Catal.* 123 (1990) 74.
- [49] E. Haque, J.W. Jun, S.N. Talapaneni, A. Vinu, S.H. Jhung, *J. Mater. Chem.* 20 (2010) 10801.